Modeling of Lightning Exposure of Buildings and Massive Structures

Farouk A. M. Rizk, *Life Fellow, IEEE*

***Abstract*—A dynamic model for exposure of grounded objects to direct lightning strokes has been generalized to apply to buildings and massive structures. The model also applies to the mixed situation where a slender air terminal is installed on the top of a building to provide lightning protection. The basic elements of the model comprise a general criterion for continuous upward leader inception the validity of which is independent of the building or structure topology. This is followed by initiation of an upward leader trajectory which would either lead to a successful encounter with the negative downward leader through a final jump or to an aborted positive leader. Based on recent work published by the author, the model does not require any assumption regarding the ratio between the negative and positive leader speeds as has often been done previously. The modeling procedure has been facilitated through the use of dimensionless variables relating to the proximity effect of the building on space potential distribution, leader inception space potential, critical mean ambient ground field, and, finally, the attractive radius. A slender rod of the same height as the building is used as basis for comparison.**

***Index Terms*—Attractive distance, critical gradient, leader discharge, lightning, protection, streamers.**

I. Introduction

LIGHTNING protection has been extensively reviewed by Golde [1] and more recently by Uman [2]. In this context, thedefinition of the protective zone around a lightning rod or sideways from an overhead ground wire is of fundamental importance.

Traditionally, such a protective zone was defined by a protective angle from the vertical, which for the ground rod determines a cone and for a ground wire describes a right rectangular wedge. The protective angle recommended for Franklin rods and, accordingly, the ratio between the protection cone base radius and the rod height varied, within a wide range [1]. Originally, these protective angles were based on experience but later with the availability of high-voltage test facilities, these angles were also determined by tests on reduced-scale physical models [3]. The more conservative the design, the smaller the protective angle that was adopted often within the range of 30°–60°.

Protective angles in the application of overhead ground wires on power transmission lines have been the subject of more extensive investigations based on mathematical modeling, calibrated to field experience with direct lightning strokes [4], [5] which led to the so-called electrogeometric model (EGM). Reviews of more recent work by CIGRE and IEEE are included in [6] and [7].

The conical protection zone with the fixed angle was not unanimously accepted; however, and as early as 1880, it was suggested by Preece [8] that the protection zone is not limited by a straight line defining the cone but rather by a circular arc. The same view was much later expressed by Schwaiger [9].

II. Rolling Sphere Method

Two significant IEEE papers on the lightning protection of buildings were written by R.H. Lee in 1978 [10] and 1979 [11]. Reference [10] was based on research work carried out by E. R. Whitehead for the Edison Electric Institute (EEI) on the mechanism of lightning flashovers of 230-kV and 345-kV transmission lines [12]. Whitehead's work confirmed that in order to fulfill a predetermined performance criterion in terms of a lightning flashover rate, smaller protective angles are required for conductors with a greater height above ground. For a 99.5% protection level, a 33° protection angle would be adequate for a conductor height of 22.9 m (75 ft), while for a 45.7-m (150 ft) height, the zero degree angle would be required. For 53.3 m (175 ft) and 61.0 m (200 ft) heights, negative shielding angles were required in order to meet the aforementioned performance criterion. In [10], Lee used a step-by-step approach to construct the profile of the protection zone from Whitehead's results on transmission lines having a basic insulation level (BIL) of 1400 kV.

It was found [10] that a circular arc of radius 45.7 m would closely define the boundary of the protection zone. Lee visualized this result by imagining a sphere of 45.7-m radius rolling over the earth surface, wall, and air terminals. Objects touched by the rolling sphere are succeptible to be struck while those not touched will be protected.

Again based on the work of Whitehead, [11] concludes that for transmission lines, the critical current increases with BIL which leads to an increase in the so-called striking distance and accordingly, the radius of the rolling sphere. Since the terms "basic insulation level" and "surge impedance" are not meaningful terms for buildings, Lee recommended a critical current of 10 kA as the threshold for damaging lightning current [11].

The rolling sphere method has been included in the NFPA 78 in 1980 and is still prominent in the NFPA 780, 2004 edition [13], with the 46-m (150-ft) sphere radius.

The rolling sphere method has also been accepted by IEC [14], which defines four protection levels of 99%, 97%, 91%, and 84% which, using CIGRE log-normal lightning stroke current distribution, corresponds to 2.9 kA, 5.4 kA, 10.1 kA, and

Manuscript received November 05, 2008. Current version published September 23, 2009. Paper no. TPWRD00819-2008.

The author is with Expodev, Inc. and Lightning Electrotechnologies, Inc., Montreal, QC H3B 3K9, Canada.

Digital Object Identifier 10.1109/TPWRD.2009.2028759

15.7 kA, respectively. Based on the following relationship between return stroke current amplitude I_o and striking distance r_s

$$r_s = 10\, I_o^{0.65} \qquad (m, kA) \tag{1}$$

the rolling sphere radii for the aforementioned protection classes become 20 m, 30 m, 45 m, and 60 m, respectively.

At the time of its introduction, the rolling sphere method certainly represented a significant improvement over the fixed-angle protection cone used previously. It is simple and easy to use over complex structures and with modern computer graphics, it is no longer necessary to build physical models of buildings or structures to be protected. With more recent advances in our understanding of discharge physics of long air gaps and consequently of the lightning attachment mechanism, however, several limitations of the rolling sphere method become apparent as follows.

- It should be clear from the above that the rolling sphere method is an offshoot of the electrogeometric model for transmission lines and there is nothing particular in the method that is specific to buildings or massive structures.
- At least in its original form, the rolling sphere method does not differentiate between the circular curves defining the protective zones of Franklin rods or overhead ground wires.
- The sphere radius is only a function of the critical current and not the height of the rod, ground wire, or the building on which air terminals are installed.
- With a constant height independent radius, the rolling sphere method ignores the role played by the air terminal or the protected object in the lightning attachment processes.
- As such, the rolling sphere method implies the same striking distance for ground, wall, building edge, building corner, or building roof which defies physical explanation [15].
- The rolling sphere method does not account for the effect of the building topology on the lightning exposure of an air terminal. For example, a 0.5-m Franklin rod installed at the roof of a 30-m high building becomes the same as a 30.5-m mast above ground.
- The basic assumption of a constant 46-m rolling sphere radius leads to particular consequences that are difficult to explain from a physical point of view. These include the concept of a "useless height" of a mast or the assertion that the vertical wall of a building is not protected for heights above 50 m. Similarly, the claim that the rolling sphere method can account for side flashes to tall masts is difficult to understand when such complex phenomena can only be satisfactorily explained if due consideration is given to space charge effects at the mast top.

III. Recent Models

The aforementioned analysis shows that there is a need to apply more recent research to model lightning exposure of buildings. In [16], the leader progression model based on the critical radius concept [17] was extended to buildings by assuming that the building corner behaves like a slim vertical rod of the same height. The cross section of the building was simulated by long cylindrical conductors of a critical radius. This attempt to consider the effect of the building topology on the attachment process certainly constitutes an advance over the rolling sphere method. However, two questions can be raised concerning:

- the accuracy of the critical radius of the sphere selected to simulate a building corner; this subject has been treated in a recent paper submitted for publication [18];
- the validity of the assertion that once an upward leader is initiated from a building corner, it will, despite the building proximity, continue to progress at the same critical ground field as that of an isolated sphere of the same height.

This problem will be dealt with in detail in this paper.

A recent model for the determination of the inception criterion of an upward connecting leader is described in [19] and applied first to a slender vertical rod and subsequently to a rectangular building. The basic point in the model is the attempt to calculate the streamer and leader corona charges by the charge simulation method. It is assumed that corona occupies a conical zone with a semiangle of 60° and that if the streamer charge exceeds 1 μC, unstable leader inception occurs and an incremental leader extension is determined. Again, the leader corona charge is calculated. If the incremental corona charge again exceeds 1 μC, it is considered that leader propagation continues. The minimum ambient ground field in which a vertical rod or a building is immersed and which permits the leader to reach 2-m length is taken as the critical or stability field [19]. The results of the stability field for a vertical rod of heights in the range of 10 m–200 m were compared to the findings of several previous models. Due to the excessive computer time, a simplified method, previously suggested by Geolian *et al.* [20], was utilized to calculate the streamer charge. Here, it is assumed that the streamer charge is proportional to the area between the space potential curve starting from the grounded rod or building and a straight line having a slope of 450 kV/m representing the mean positive streamer gradient.

With respect to the Becerra–Cooray model [19], it should be noted that:

- the complex structure of the streamer zone, including its filamentary nature, branching, etc. [24], together with the fact that most of the charge resides in discrete filament tips, make accurate calculations of streamer charge extremely difficult if at all possible; the level of accuracy required will be more prohibitive if the criterion for continuous leader propagation depends on incremental corona charge variations due to small extensions in the leader length as accomplished in [19].
- the selection of a conical zone with a 60° semiangle to represent the streamer discharge or leader corona will have a major influence on the charge determined by the charge simulation method and could only be accepted as a crude simplification; it is also not clear why the semiangle of the leader corona zone will be maintained during leader propagation.
- the 1-μC streamer charge, which is taken to determine unstable leader formation or as a criterion for continuous leader propagation, has not been physically justified; the

measured corona charge in laboratory gaps in the vicinity of the inception voltage level was not found to be constant but varied with inception voltage as well as with the geometry of the high-voltage electrode and the gap length [21];

- the proportionality assumed between the streamer charge and the area between the space potential curve and the streamer gradient line has not been rigorously proven [20]; in fact, the distortion of the space potential curve due to streamer space charge is not confined to this zone;. while the electric field will be reduced in the corona zone, it certainly will be enhanced outside that zone. Furthermore, the accuracy of the method has not been validated experimentally;
- for a vertical rod, the comparison of the stabilization fields, calculated from different models, shows large dispersion [19]; Rizk's model [22] yields the lowest values for the critical (stabilization) field with Petrov and Walters [23] giving the highest values;
- the so-called striking distance studied in [19], characterizing the position of the negative descending leader when an upward (continuous) leader is initiated from a structure, does not guarantee that the structure will be struck. This can only be determined when the subsequent trajectory of the upward connecting leader is investigated to ensure an encounter with the negative descending leader in a final jump; this latter situation has been described by the maximum attractive radius around a mast or maximum lateral attractive distance from a ground wire [25], [26];
- in comparison with the aforementioned, the critical conditions for continuous leader inception in Rizk's model are [30]:
  - — a critical streamer or leader corona charge $\mathrm{Q_o}$, which is not constant, but assumed to be proportional to the continuous leader inception voltage $U_{\ell c}$; this means that a ratio $\mathrm{Q_o}/U_{\ell c}$, which has the dimension of capacitance, is assumed to characterize the critical streamer size;
  - — simultaneously, the net electric field at the leader tip, due to the applied voltage and the leader corona space charge and its ground images, must exceed a critical value $\mathrm{E_c}$ in order to maintain leader propagation; this critical value is far higher than the mean streamer gradient $\mathrm{E_s}$; otherwise, any streamer filament which extinguishes could not be replaced [36];
  - — it has been emphasized in Rizk's model [30] that the complex leader corona is not for all purposes replaced by a point charge but that only as far as the voltage induced by the leader corona charge at the leader tip position, a charge $\mathrm{Q_o}$ is placed at an equivalent center of charge, a distance s from the leader tip, with s being independent of the gap length.
  - — the formula for continuous leader inception obtained in [30] was found to be identical to that following analysis of the situation at the final jump [29]; this would not be the case if $\mathrm{Q_o}$ were assumed constant.

Experimental results of the onset of a continuous leader from a tall mast under a large plane electrode simulating an upward connecting leader [27], [28] have been re-examined in [18]. It was shown that when the proximity effect of the plane is properly limited, there is no significant difference between such conditions and those prevailing during high-voltage testing of large air gaps and could be closely predicted by Rizk's model [29]. It is therefore possible and even desirable to compare mathematical models for upward leader inception not among themselves but with experimental results of corresponding tests on large air gaps in high-voltage laboratories. A 10-m rod-plane gap has been extensively tested under positive critical switching impulse in the laboratory. For a 10-m rod-plane gap [29] yields a continuous leader inception voltage of 1120 kV, corresponding to a mean critical ground field of 112 kV/m. The procedure of [29] results in a 50% breakdown voltage of 1833 kV while the empirical value from the well-known CRIEPI formula

$$\mathrm{U_{50}} = 1080 \ln(1 + 0.46\,\mathrm{h}) \qquad (\mathrm{kV, m}) \tag{2}$$

with h being the gap spacing or rod height, is obtained at $\mathrm{U_{50}} =$ 1861 kV, which differs from the experimental value by 1.5%.

If we apply the same procedure to the ground field of 240 kV/m quoted in [19] for the Petrov and Waters model [23], the continuous leader inception voltage of a 10-m laboratory gap would be 2400 kV, which is already far beyond the 50% breakdown voltage. The critical leader stability field of the 10-m rod from the Becerra and Cooray model [19] amounts to 175 kV/m, corresponding to a continuous leader inception voltage of 1750 kV for a 10-m laboratory gap, which is quite excessive.

It is also noted that with a combination of testing and calculations, Carrara and Thione [17] determined for a 10-m gap, a critical radius of 34 cm and a continuous leader inception voltage of 1108 kV, corresponding to a mean critical (stability) ground field of 110.8 kV/m in close agreement with the value of 112 kV/m obtained from Rizk's model [29] as shown before.

The excessive critical ground field of approximately 175 kV/m obtained by Becerra and Cooray [19] for the same configuration can be understood to be a consequence of the oversimplifications and selection of parameters of their model. Other publications by Becerra and Cooray [31], [32] while producing different numerical values, did not address the basic limitations of the model noted before.

S. Ait-Amar and G. Berger formulated a model for the attractive radius of a building [33] and later used the model to propose modifications to the rolling sphere method [34]. The electric field was determined by the finite-element method in the vicinity of a lightning rod, a corner, or an edge of a building. The fundamental assumption of the model is that upward leader inception takes place from any of these points of the building when the electric field at 1-m distance from the point reaches 500 kV/m, which has not been physically justified. In order to verify this assumption, consider a 10 m sphere-plane gap for which Carrara–Thione [17] determined a critical radius of 34 cm and a continuous leader inception voltage of 1108 kV. At this voltage, the electric field at a distance 1 m from the sphere along the axis was determined by charge simulation at only 217 kV/m. Ait-Amar and Berger requirement of a field of 500 V/m at 1-m distance would result in a continuous leader inception voltage of 2553 kV instead of the experimental value of 1108 kV.

Following upward leader inception, leader trajectories are constructed for different ratios of negative to positive leader speeds as was reported earlier by Rizk in [25]. These authors confirmed the vulnerability of building corners and edges. This justifies a more extensive investigation of the criterion for upward leader inception from such locations, which will be carried out in this paper.

IV. Model Formulation

In [30], the author has previously formulated a general criterion for continuous positive leader inception voltage in long air gaps

$$U_{\ell c} = \frac{U_{c\infty}}{1 + \frac{A}{R}} \tag{3}$$

where $U_{c\infty}$ is a constant saturation value of $U_{\ell c}$ for very large gaps, with 1556 kV for rod-type and 2247 kV for conductor-type high-voltage electrodes. For the former electrode type, A is a constant while for the latter, A varies slightly with the conductor radius. R is a function of the electrode and the gap geometry and can be determined analytically for simple gaps, amounting to 2 h for a rod of height h above ground. For more complex high-voltage and ground electrodes, R can be determined by the charge simulation method [35] from the voltage induced in the vicinity of the high-voltage electrode by the images of the equivalent streamer charge on the ground electrode. The model has been extended to account for the lightning attachment process from slender structures [25], where the definition the equivalent radius of the structure is much smaller than its height above ground. A major objective of this paper is to explore the possibility of generalizing this model to apply to buildings and massive structures where the slenderness condition does not apply. This generalization should also cover the mixed situation where a slender air terminal is installed atop a building or massive structure. Paradoxically, this mixed situation is easier to understand and will therefore be treated first. An improvement over the basic model described in [25] is that instead of assuming a constant ratio between the negative and positive leader speeds, the leader speeds are considered to vary with the tip overvoltage factor or with the dynamic leader current as reported by Rizk and Vidal [36].

Another modification is that the quasistationary leader gradient E_{∞} assumed constant in [25] is here taken as a function of the leader current [22]. All of these variables are evaluated continuously during leader propagation, as will be described elsewhere in greater detail.

V. Air Terminal on Building Top

For simplicity, consider a slender air terminal of height h installed centrally on the roof a of a tall cylindrical steel structure building with diameter D and height H (Fig. 1). In general, charges will be induced on the building and on the rod due to cloud charges producing an ambient ground field $\mathrm{E_g}$ or due to charges associated with a downward stepped leader. The latter charges are normally related to the prospective return stroke current magnitude.

As a starting point for comparison, let us consider a slender rod of the same height $\mathrm{H+h}$ above ground. Here, the continuous

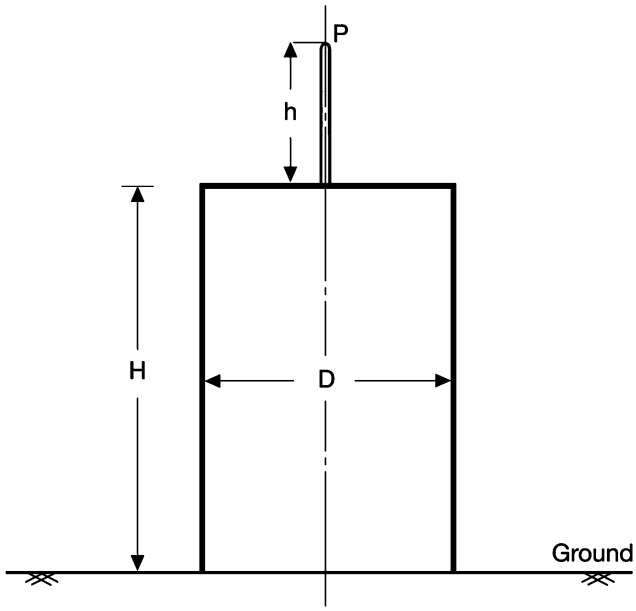

Fig. 1. Lightning mast at the roof center of a tall cylindrical building.

leader inception voltage is straightforward and according to (3), is given by [30]

$$U_{\ell \mathrm{co}} = \frac{1556}{1 + \frac{3.89}{(\mathrm{H+h})}} \quad (\mathrm{kV, m}). \tag{4}$$

Let the space potential at the rod tip position, in the absence of the rod, required for continuous leader inception be designated U_{sco}.

In general

$$U_{\mathrm{sco}} = \int_{o}^{\mathrm{H+h}} E_{\mathrm{gco}}(\mathrm{z})\mathrm{dz} \tag{5}$$

where E_{gco} (z) describes the ambient field distribution required to produce the critical value U_{sco}.

For the simple case of an assumed uniform ambient ground field E_{gco} over the distance $\mathrm{H + h}$

$$U_{\mathrm{sco}} = E_{\mathrm{gco}}(\mathrm{H + h}). \tag{6}$$

If the field varies with z along the distance $\mathrm{H + h}$, E_{gco} in (6) would then refer to the mean value of the field along that path. Equating (4) and (6)

$$E_{\mathrm{gco}} = \frac{1556}{H + h + 3.89} \qquad (\mathrm{kV/m, m}). \tag{7}$$

Now back to the building of Fig. 1, from (3) before, the continuous leader inception voltage $U_{\ell \mathrm{c}}$ of the rod will be influenced by the proximity of the massive building which affects the function R.

This proximity effect will obviously depend on the dimensions H, D, and h and can be defined by a leader inception proximity factor K_{ℓ} defined by

$$\mathrm{K}_{\ell} = \frac{U_{\ell \mathrm{c}}}{U_{\ell \mathrm{co}}} \tag{8}$$

which follows from finding $U_{\ell c}$ once the function R has been determined by the charge simulation technique. In general, building proximity will also tend to suppress the space potential $\mathrm{U_s}$ at the rod tip position P in Fig. 1 so that

$$\mathrm{U_s} = \mathrm{K_{sp}} \cdot \mathrm{U_{so}} \tag{9}$$

where $\mathrm{K_{sp}}$ is a space potential proximity factor, and $\mathrm{U_{so}}$ is the space potential that would have existed in the absence of the building. The simple case of a uniform ambient ground field is instructive, yielding the following relationship between the critical ground field E_{gc} in the presence of the building and E_{gco} for a slender rod of equal total height

$$E_{\mathrm{gc}} = \frac{\mathrm{K}_\ell}{\mathrm{K_{sp}}} \cdot E_{\mathrm{gco}} \tag{10}$$

with E_{gco} expressed by (7).

It should be noted that for buildings and massive structures, as will be shown numerically, $\mathrm{K}_\ell < 1, \mathrm{K_{sp}} < 1$ and $\mathrm{K_{sp}} < \mathrm{K}_\ell$ so that the critical ambient ground field for an air terminal on the roof of a building will always be higher than that of a corresponding rod of the same total height above ground. More generally, the effect of the building on the required critical continuous leader ambient space potential at the rod tip position can be expressed as

$$U_{\mathrm{sco}} = \frac{\mathrm{K}_\ell}{\mathrm{K_{sp}}} \cdot U_{\ell co}. \tag{11}$$

As a numerical example, consider a cylindrical building with a height $\mathrm{H} = 100$ m, a diameter $\mathrm{D} = 40$ m, and a lightning rod with $\mathrm{h} = 10$ m installed at the center of the roof. The building is immersed in a uniform ambient ground field $\mathrm{E_g} = 20$ kV/m due to cloud charges. By charge simulation, the space potential $\mathrm{U_s}$ at the position P of the rod tip (Fig. 1) amounts to 733.7 kV. The space potential $\mathrm{U_{so}}$ for the same $\mathrm{E_g}$ in the absence of the building amounts to 2200 kV, yielding a space potential proximity factor $\mathrm{K_{sp}}$ of 0.334.

The function R for the 10-m air terminal in the presence of the building was obtained by charge simulation as 28.2 m (compared to 20 m for a 10 m rod above ground), which from (3) yields a continuous leader space potential of 1219.5 kV. Without the building, the leader inception voltage $U_{\ell \mathrm{co}}$ of a 110-m rod above ground is 1502.9 kV [30], corresponding to a critical ground field $E_{\mathrm{gco}} = 13.7$ kV/m. It follows that the leader inception proximity factor $\mathrm{K}_\ell = 0.8115$.

From (10), the critical ambient ground field (stability field) for the 10-m rod at the 100-m building top becomes

$$E_{\mathrm{gc}} = \frac{0.8115}{0.334} \bullet 13.66 = 33.2 \text{ kV/m}.$$

This compares with a 112-kV/m critical field for a 10-m rod on the ground plane as shown before. The same procedure was repeated with the space potential determined due to a descending leader at different positions from the building, where the assumption of a uniform ambient ground field would be inaccurate.

For a downward leader tip at a 100-m radial distance from the building axis and 200 m above ground (i.e., 100 m above the roof and with a prospective return stroke current $\mathrm{I_o} = 12$ kA, a cloud height $\mathrm{H_{c1}}$ of 2000 m and a downward leader charge distribution as in [25], the space potential $\mathrm{U_s}$ at the 10-m rod tip position amounted to 874.3 kV. In the absence of the building, the downward leader charge resulted in a space potential $\mathrm{U_{so}} = 2537$ kV, yielding a space potential proximity factor $\mathrm{K_{sp}} = 0.345$. This is close to the value of 0.334 obtained above for a uniform ambient ground field. For a negative leader descending along the building axis and a 200-m-high leader tip, with the same prospective return stroke current of 12 kA, $\mathrm{U_s} = 1086.6$ kV, and $\mathrm{U_{so}} = 3160$ kV, the result is a space potential proximity factor $\mathrm{K_{sp}}$ of 0.344. This and other calculations confirm that for the same building dimensions and position of the air terminal tip, the space potential proximity factor $\mathrm{K_{sp}}$ is rather insensitive to the position of the downward leader, at least for positions that are relevant to the inception of an upward connecting leader.

Following continuous leader inception, the upward connecting leader starts on a trajectory to meet the downward stepped leader [25]. Depending on the position of the downward stepped leader at the instant of upward leader inception and to the subsequent relative speeds of the two leaders (generally variable), this may lead to either an encounter in a final jump or to an aborted positive leader. For any prospective return stroke current, the maximum radial distance allowing a successful encounter is called the attractive radius $\mathrm{r_a}$ of the air terminal [25].

For the aforementioned case with $\mathrm{I_o}$ =12 kA, a 110-m-high rod above ground resulted in an attractive radius of 95.1 m, while on a 100-m building, the 10-m rod had an attractive radius of only 72.6 m. This shows that the building proximity has a significant effect in reducing the attractive radius of an air terminal. In this sense, the building is also shielding the lightning rod.

There still appears to be considerable confusion in the literature regarding the term "striking distance," which has been attributed to Franklin and used by Golde [1].

In [25], a distinction has been clearly made between three distances associated with the attachment process, see Fig. 2, as follows.

$\mathrm{d_i}$ is the distance between the negative leader tip and structure (rod) or conductor at a continuous upward positive leader inception. This distance should not be confused with the striking distance [19].

$\mathrm{d_s}$ is the striking distance defined as the distance between the structure and negative leader tip at the critical point of encounter. It is at this point that the negative descending leader (or branch) abruptly changes orientation in a final jump towards the upward connecting leader.

$\mathrm{r_a}$ is the maximum attractive radius as defined before and which again is different from the striking distance.

For the aforementioned example of a 10 m mast on the 100 m cylindrical building with $\mathrm{I_o} = 12$ kA, the present model yields $\mathrm{d_i} = 132.6$ 132.6 m, $\mathrm{d_s} = 76.7$. and $\mathrm{r_a} = 72.6$ m.

The aforementioned approach is general and not restricted to either cylindrical buildings nor to air terminals placed along any axis of symmetry. For any building configuration and any height and position of an air terminal, the space potential proximity factor $\mathrm{K_{sp}}$ and the leader inception proximity factor K_ℓ are

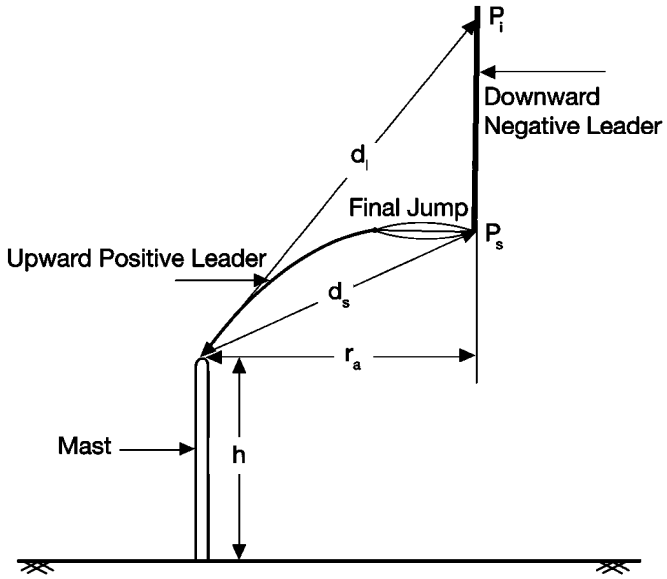

Fig. 2. Schematic diagram of the lightning attachment process in a critical encounter according to the model, corresponding to the maximum attractive radius r_a.

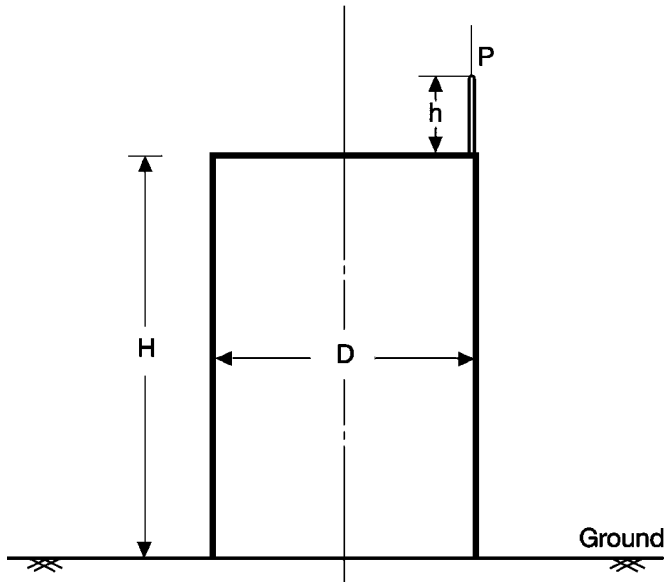

Fig. 3. Air terminal at the roof edge of a tall cylindrical building. Only one lightning rod is shown.

found by charge simulation or finite elements methods and then the continuous leader inception space potential is determined from (11) before.

As an example, consider a 2-m lightning rod installed at the roof edge of the above cylindrical building with 100-m height and 40-m diameter, Fig. 3. Consider again a downward leader with 80-m radial distance from and 98 m above the rod tip. For a prospective return stroke current $I_o = 12$ kA and a cloud base height of 2000 m, the space potential U_s at the position of the rod tip amounts to 447.7 kV. In the absence of the building $U_{so} = 2485$ kV, yielding a building space potential proximity factor K_{sp} of 0.1802. It is obvious that the building proximity effect here for the 2-m rod is much more substantial (i.e., a lower space potential proximity factor) than for the 10-m rod.

The function R was determined at 4.65 m (compared to 4 m for a 2 m rod above ground) resulting in a continuous leader inception space potential of 582.1 kV in the presence of the building, corresponding to a local mean voltage gradient of 291 kV/m. For a 102-m rod above ground $U_{\ell co} = 1498.8$ kV, which gives a leader inception proximity factor $K_\ell = 0.388$. Therefore, the continuous leader space potential U_{sco} defined by (5) above and using (11) was determined at 3227 kV, corresponding to a mean ambient critical ground field $E_{gc} = 31.6$ kV/m. This compares to $E_{gco} = 14.7$ kV/m for a 102-m slender rod above ground and to a critical ground field of 260 kV/m for a 2-m rod on the ground plane. Using the dynamic upward leader trajectory as explained in [25], the attractive radius of the 2-m air terminal on the building for $I_o = 12$ kA amounts to 73.4 m. This compares with $r_a = 93.1$ m for a 102-m air terminal above ground and $r_a = 25.1$ m for a 2-m slender rod on ground plane, all for $I_o = 12$ kA. This demonstrates the importance of accounting for the effect of building proximity on the attractive radius of an air terminal and puts into question the use of a rolling sphere with a constant radius that only depends on the prospective return stroke current.

TABLE I
SUMMARY OF ATTRACTIVE DISTANCE RESULTS FOR CYLINDRICAL BUILDING H = 100 m, D = 40 m

I_o, kA	Air Terminal	Maximum Attractive Distance, m
12	10m Rod Roof Center	72.6
	110m Rod on Ground Plane	95.1
	10m Rod on Ground Plane	40.5
12	2m Rod at Roof Edge	73.4
	102m Rod on Ground Plane	93.1
	2m Rod on Ground Plane	25.1

A summary of the above numerical results is given in Table I.

VI. GENERAL CRITERION

It is well known that building corners and roof edges are the most vulnerable locations for lightning strikes [37]. As usual, it is assumed that the structure is electrically conducting and grounded. Fig. 4 shows a schematic diagram of a roof edge where a gradual transition is made from the wall to the roof through a surface with an arbitrarily small radius of curvature, to avoid electric-field discontinuity.

Due to structural details as well as protrusions, water drops etc. conditions for streamers and short unstable leaders are first met either due to the ambient ground field caused by cloud charges or due to a remote downward stepped leader. A more stringent requirement is that of the formation of a continuous upward leader.

In order to formulate these conditions, consider Fig. 4., where a line with an angle α to the horizontal characterizes the path of steepest increase in the space potential (maximum gradient) away from the building edge. This line can be determined by electric-field calculations. For continuous leader propagation, the tip position P of a leader of any length ℓ (usually in the few

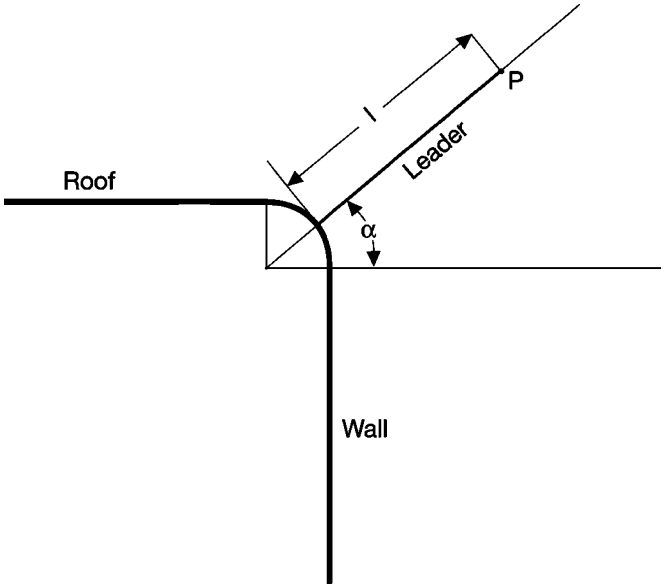

Fig. 4. Schematic diagram illustrating leader inception from the roof edge.

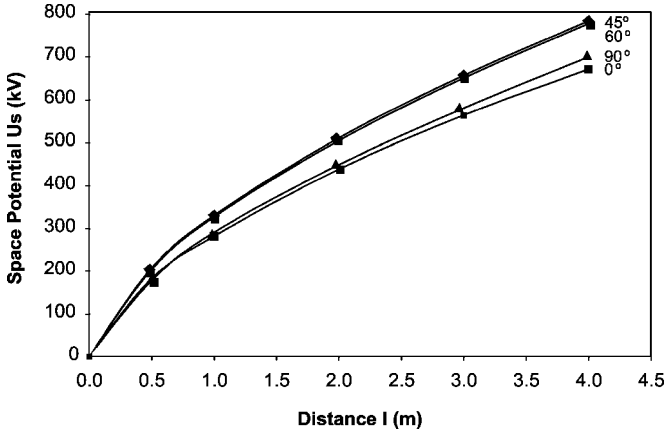

Fig. 5. Variation of the space potential at the roof edge along different slope lines. Building: H = 100 m, D = 40 m. Leader (100 m, 200 m), I = 12 kA.

meter range) is required; in the building vicinity, the criterion for continuous leader inception is satisfied. Otherwise, the leader will be aborted.

Following the approach outlined in the previous section, with due consideration to the building proximity effect, let the space potential at point P be $U_{\rm s}(\ell)$ as produced by cloud charges and/or descending leader charge.

Also with due consideration to building proximity through proper determination of the function R, let the continuous leader inception voltage at the tip P be $U_{\ell c}(\ell)$.

A leader of length ℓ will have a voltage drop $\Delta U(\ell)$, which can be determined as described in [29].

The criterion for continuous leader propagation at any length ℓ will therefore be

$$U_{\rm s}(\ell) - \Delta U(\ell) \geq U_{\ell c}(\ell). \tag{12}$$

Let the proximity factor be Ksp and the continuous leader inception proximity factor be k ℓ. For the determination of k ℓ, the base quantity $U\ell$ co refers to a free-standing rod of the same height as the building. Substituting in (12), the criterion for continuous leader propagation becomes

$$K_{\rm sp}U_{\rm so}(\ell) \geq K_\ell U_{\rm lco} + \Delta U(\ell). \tag{13}$$

If it is required to express this criterion in terms of a mean critical ambient ground field $E_{\rm gc}$, considering the height z (ℓ) of the point P above ground

$$K_{\rm sp} \cdot E_{\rm gc} \cdot z(\ell) = K_\ell \cdot U_{\ell \rm co} + \Delta U(\ell)$$

or

$$E_{\rm gc} = \frac{K_\ell}{K_{\rm sp}} \cdot \frac{U_{\ell \rm co}}{z(\ell)} + \frac{\Delta U(\ell)}{K_{\rm sp} \cdot z(\ell)}. \tag{14}$$

In terms of the critical ground field $E_{\rm gco}$ of a slender rod of the same height as the building, (14) could be written as

$$E_{\rm gc} = E_{\rm gco}\left[\frac{K_\ell}{K_{\rm sp}} + \frac{\Delta U(\ell)}{K_{\rm sp} \cdot U_{\ell \rm co}}\right]. \tag{15}$$

In (15), $\rm K_\ell, K_{sp}$ and $\Delta U(\ell)$ are all sensitive to the leader length ℓ while $U_{\ell \rm co}(\ell)$ is basically determined by the height of the building.

Accordingly, ℓ will be varied in steps in order to determine the maximum value of $E_{\rm gc}$, which will then characterize the roof edge in question.

A convenient overall proximity factor, which accounts for the building effect on the space potential and the continuous leader inception voltage is defined as

$$\rm K_p = \frac{U_{sco}}{U_{\ell co}} = \frac{E_{gc}}{E_{gco}} = \frac{K_\ell}{K_{sp}} + \frac{\Delta U(\ell)}{K_{sp} \cdot U_{\ell co}}. \tag{16}$$

By definition for a slender rod above ground plane $\rm K_\ell = 1, K_{sp} = 1$ (in the absence of the rod) and $\rm \Delta U = 0$ so that $E_{\rm gc} = E_{\rm gco}$ and the overall proximity factor $\rm K_p = 1$, which is to be expected since the slender rod is used as the base case for comparison.

VII. Building Edges

The general criterion developed above will be made clearer by specific examples.

Consider again, a cylindrical building with a height of 100 m and a diameter of 40 m (i.e., H/D = 2.5). Also consider a downward leader 100 m from the building axis and a leader tip 200 m above ground with a prospective return stroke current of 12 kA. The cloud base is 2000 m above ground. Fig. 5 shows a variation of the space potential at the roof edge for different slope lines from $\alpha = 0$ (horizontal) to $\alpha = 90°$ (vertical). It is shown that the steepest rise of space potential occurs along the 45° line. Fig. 6 shows the variation of the mean critical ground field for continuous leader inception from the building edge for different positions along the 45° line, yielding a maximum of 38 kV/m for ℓ slightly above 2 m. This compares with a mean critical ground field of only 15 kV/m for a slender 100-m rod above the ground plane.

In order to account for the effect of the building height for a constant building diameter of 40 m, Fig. 7 shows the dependence of the overall building proximity factor $\rm K_p$ on the building height in the range of 20 m—100 m. It is shown that the inhibiting effect of the building on continuous leader inception,

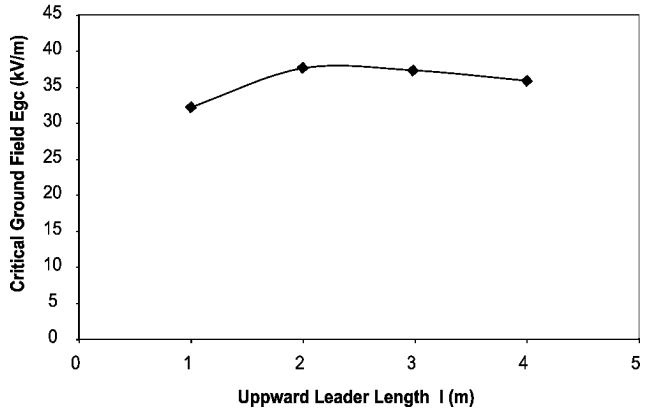

Fig. 6. Variation of the mean critical ground field due to downward leader charge at different upward leader lengths. Cylindrical building: h = 100 m, D = 40 m.

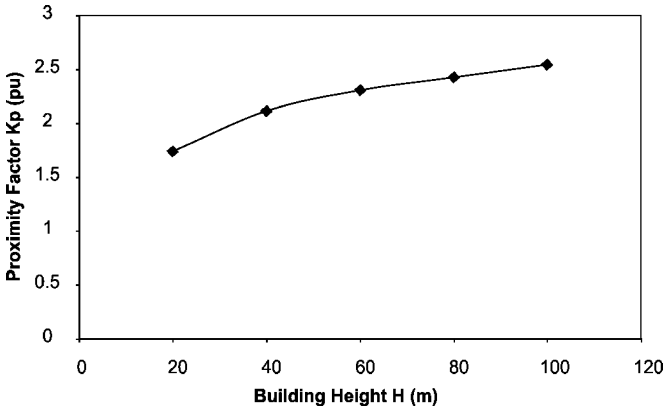

Fig. 7. Variation of overall proximity factor Kp with cylindrical building height. Building diameter: 40 m.

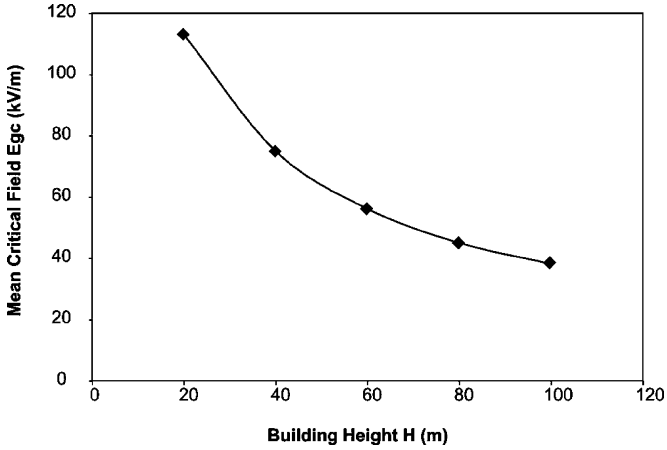

Fig. 8. Variation of continuous leader inception mean ground field E_{gc} with cylindrical building height. Cylinder diameter: 40 m.

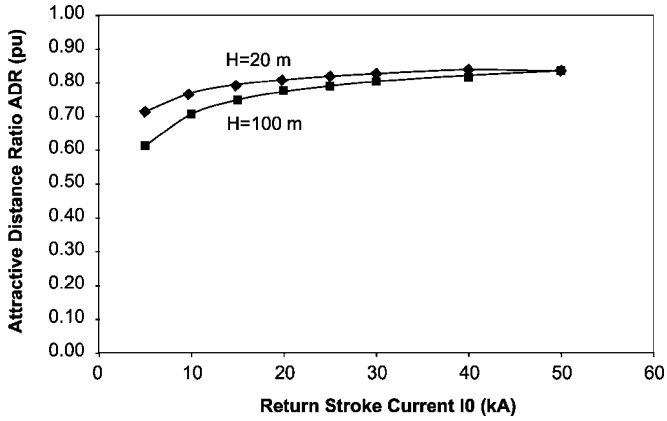

Fig. 9. Variation of attractive distance ratio of the cylindrical building edge with prospective return stroke current.

compared to a slender rod of the same height, increases with building height although the rate of increase is higher for the 20-m building than for the 100-m building. Fig. 8 shows variation of the mean ambient critical ground field for continuous leader inception with building height for buildings with 40-m diameter. It is shown that the critical ground field E_{gc} increases from 38 kV/m for a 100-m building to 113 kV/m for a 20-m building. For comparison, the mean critical ground field of a 20-m slender rod on the ground plane is determined by the model at 65 kV/m.

As previously mentioned, the ultimate goal of the model is not to determine the conditions for continuous upward leader inception but to obtain the maximum attractive distance. Since the attractive distance (radius) of slender rods has been extensively studied in the literature [25], [26], a convenient dimensionless parameter is here introduced. The attractive distance ratio (ADR) is defined as the ratio between the attractive distance of a complex structure (building) edge or corner and that of a slender rod of the same height. Fig. 9 shows the variation of the attractive distance ratio (ADR) on prospective return stroke current in the range 5 kA to 50 kA for cylindrical buildings of 40-m diameter and heights of 20 m and 100 m. Here, the initial ground field due to cloud charges is 10 kV/m. It is noted first that the reduction of the attractive distance is slightly more significant for the 100-m building. Second, the ADR increases with a prospective return stroke current reaching 0.84 at 50 kA.

More interestingly, at an assumed threshold current of 10 kA and for building heights in the range 20–100 m, ADR varies in the limited range of 0.71 to 0.77 p.u., corresponding to a reduction in the attractive distance due to a building proximity of 23% to 29% or by a mean value of approximately 25%.

Table II includes a comparison between the maximum attractive distance of a 100-m cylindrical building, having a 40-m diameter, with the attractive distances of different air terminals, for a prospective return stroke current of 12 kA.

TABLE II
COMPARISON OF DIFFERENT AIR TERMINALS ON CYLINDRICAL BUILDING: H = 100 m, D = 40 m, H_{c1} = 2000 m

I_o, kA	Struck Object	Maximum Attractive Distance, m
12	10m Rod at Roof Center	72.6
	2m Rod at Roof Edge	73.4
	0.3m Rod at Roof Edge	64.5
	Roof Edge	67.2

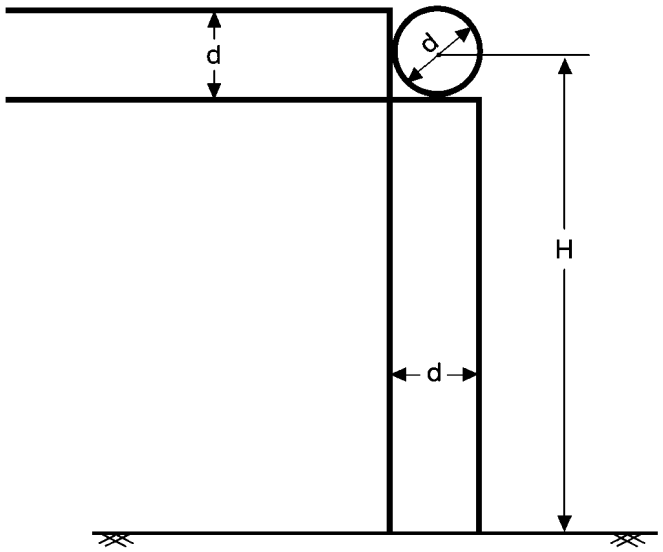

Fig. 10. Schematic diagram of the corner of a structure with dimensions L*W*H (height) of three perpendicular beams and the sphere of diameter D.

With a 20-m building radius, the attractive area of the 10-m rod at the roof center extends 52.6 m around the building, which is below the attractive distance of the edge, amounting to 67.2 m, showing that such a rod would be inadequate. The 2-m rod at the building edge on the other hand has an adequate attractive distance of 73.4 m. A 0.3-m rod corresponding to the minimum height recommended in NFPA 780 [13] has a 64.5-m attractive distance which is unsatisfactory.

VIII. Structural Corner

Fig. 10 shows a schematic diagram of the corner of a box-type structure with overall dimensions $\mathrm{L}_{*}\mathrm{W}_{*}$ H(m). The corner results from the intersection in right angles of three cylindrical beams of diameter d each and a sphere of the same diameter.

As an example, a $80{*}40{*}80$–m structure is exposed to charges of a downward leader with a 100-m radial distance from the roof corner and tip height of 200 m above ground. The prospective return stroke current $\mathrm{I_o}$ considered is 12 kA. Again, the relationship between the leader charge and return stroke current as well as the spacial distribution of the leader charge is identical to that adopted in [25].

Fig. 11 shows a variation of the space potential in the vicinity of the roof corner along lines of different angles from the horizontal of 0°, 45°, 60°, and 90° (vertical). First, this and similar calculations show that under identical conditions, the space potential rise is steeper for a corner than for an edge of a building. Second, for distances of 0.5 to 4 m from the corner, the 45° line presented the steepest space potential rise, which is then used to determine the mean critical gradient E_{gc} for continuous leader inception. Furthermore, it was found here that the requirement that the upward connecting leader reaches 3 m in length ℓ represented the most critical situation for the determination of E_{gc}.

Fig. 12 shows a variation of the mean critical gradient E_{gc} for continuous leader inception with the corner height above ground, for the $80 * 40 * \mathrm{H}$ (m) structures with H varying in

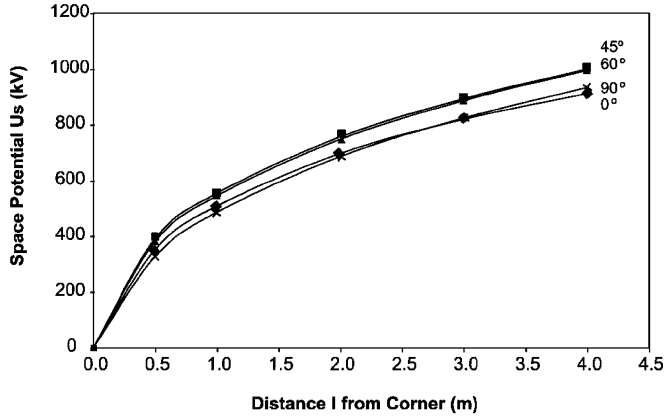

Fig. 11. Variation of the space potential in corner vicinity along different slope lines. Structure: $80{*}40{*}80{*}$m(H). Leader (100 m, 200 m), $\mathrm{I0} = 12$ kA.

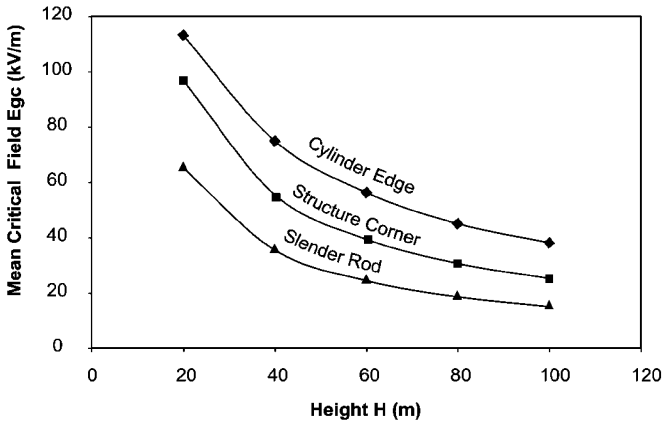

Fig. 12. Dependence of continuous leader inception mean critical ground field on height.

the range 20-100 m. For comparison, Fig. 12 also includes E_{gc} results for the edge of a 40-m cylindrical building and for a free-standing slender rod, all with the same height above ground. It is clear from Fig. 12 that a slender rod requires the lowest mean critical field for continuous upward leader inception, followed by the corner, while the building edge is the least critical. At a 100-m height, E_{gc} values for the slender rod, corner, and edge amount to 15 kV/m, 25 kV/m, and 38 kV/m, respectively. For a 20-m height, the corresponding mean critical fields for the slender rod, corner, and edge amount to 65 kV/m, 97 kV/m, and 113 kV/m, respectively.

Fig. 13 shows a variation of the attractive distance (radius) ratio ADR of a corner with 20-m and 100-m height for a return stroke current range of 5 kA to 50 kA. It is shown that the attractive distance ratio increases slowly with the return stroke current but is practically independent of the corner height above ground. If a threshold return stroke current of 10 kA is adopted, an ADR of 0.85 is obtained (i.e., the attractive radius of the corner is approximately 15% lower than the attractive radius of a slender rod of the same height), compared to a 25% reduction for a building edge as shown in the previous section. For a threshold current of 5 kA, on the other hand, the attractive radius reduction will be approximately 20% for a corner, 30% for an edge 20 m above

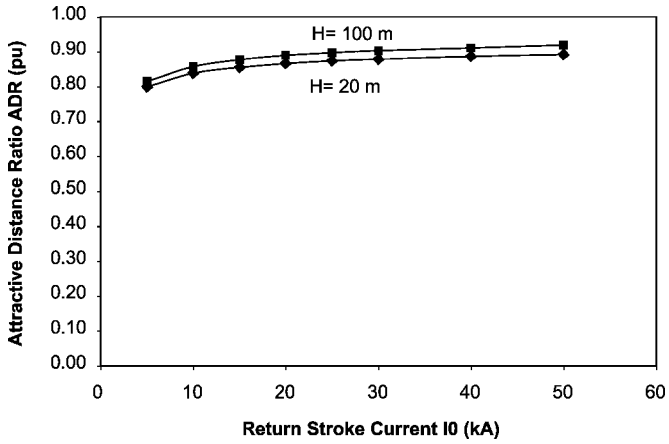

Fig. 13. Variation of an attractive distance ratio of a structure corner with return stroke current.

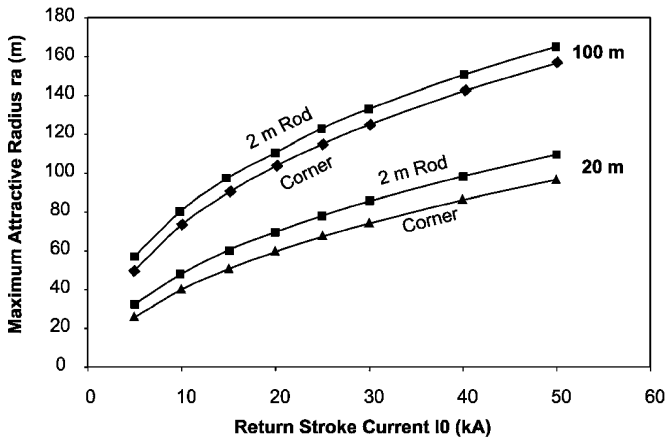

Fig. 14. Dependence of maximum attractive radius on return stroke current.

ground, with $\mathrm{H/D} = 0.5$ and 40% for an edge 100 m above ground, with $\mathrm{H/D} = 2.5$, as shown in Figs. 9 and 13.

The protective effect of a 2-m air terminal installed at structural corners 20 m and 100 m above ground is demonstrated in Fig. 14, for return stroke currents in the range 5 kA to 50 kA. It is shown that the 2-m rod provides adequate protection for both corners over the whole return stroke range and that the margin of protection (i.e., the difference between the attractive radii of the air terminal and that of the corner) is more favorable for the corner of lower height. Such protection, however, will always be assured only if the lightning rod does not tend to occasionally self-protect. This aspect will be treated in a separate publication.

IX. Model Validity

The general validity of the model described in this paper, which has so far been devoted to buildings and massive structures, was verified by applying the model to slender rods. The results were then compared to the model formulated previously [22], [25] for slender rods and conductors. The slender rods used for this investigation were hemispherically caped with 10-cm diameter and heights of 20 m and 100 m. The mean critical ambient field for continuous leader inception was determined by finding the proximity factors $\mathrm{K_{sp}}, \mathrm{K_{\ell}}$, and $\mathrm{K_p}$ as explained before. The positive upward leader trajectory followed and the attractive radius of the rod was determined through an iterative process in the usual manner. The results were then compared with those from the procedure of [22] and [25]. All calculations were made, as has been done throughout this paper, with a cloud base height of 2000 m and ground field due to cloud charges of 10 kV/m.

TABLE III
Summary of Results for Model Application to Slender Rods

Rod Height, m	Critical Ambient Field E_{gc}, kV/m		I_o, kA	Attractive Radius, m	
	Present Model	[22], [25] Approach		Present Model	[22], [25] Approach
20	65.8	65.1	10	47.2	47.4
			50	108.7	109.0
100	16.6	15.0	10	83.5	85.2
			50	168.3	170.2

The close agreement in Table III confirms the general validity of the present approach independent of the structure geometry.

X. Conclusion

A dynamic model for the exposure of rods and conductors to direct lightning strokes previously formulated by the author has been generalized to apply to buildings and massive structures. In this paper, it has been recognized that building proximity will affect the space potential distribution resulting from cloud charges and charge distribution along a downward negative leader. It has also been recognized that for an air terminal atop, a building or massive structure, the proximity effect will have a significant influence on the continuous leader inception conditions.

For building edges and corners, it has been further recognized that in practical field conditions, streamer and aborted short leader onset conditions will be met long before the criterion for the continuous leader propagation is satisfied. The latter more stringent situation requires that for any leader length in the building vicinity, conditions for continuous leader inception are satisfied. The resulting criterion stipulates that the space potential at the tip position of any leader length must exceed the sum of the leader inception voltage of a rod of the same length and the corresponding leader voltage drop.

Continuous upward leader inception in the building vicinity does not ensure that a building or an air terminal will be struck. This will only occur after a successful encounter of the upward and downward leaders through a final jump.

This paper reports, for the first time, on modeling results of the whole attachment process of a building or massive structure, together with practical applications.

Within the ranges of the parameters investigated, specific conclusions have been reached as follows.

1) Building proximity can be conveniently generalized by a space potential proximity factor $\mathrm{K_{sp}}$, which expresses the ratio between the space potential at any point in presence and in the absence of the building.
2) The space potential proximity factor depends on building geometry and location of the point concerned relative to the building.

3) The space potential proximity factor is rather insensitive to the nonuniformity of the ambient field or the position of the downward leader.
4) The continuous leader inception space potential of a rod in proximity to a building or massive structure can be conveniently related to the corresponding value for a slender rod of the same total height above ground, through a leader inception proximity factor K_{ℓ}.
5) It has been shown that for a building or massive structure $\mathrm{K}_{\mathrm{sp}} < 1, \mathrm{K}_{\ell} < 1$ and $\mathrm{K}_{\mathrm{sp}} < \mathrm{K}_{\ell}$.
6) For a building edge, corner, or air terminal on the building, the mean critical ambient field for continuous leader inception E_{gc} can be related to the corresponding value E_{gco} of a slender-free standing rod of the same total height through an overall proximity factor K_{p}, which is always greater than unity.
7) For air terminals, the overall proximity factor K_{p} is equal to the ratio $\mathrm{K}_{\ell}/\mathrm{K}_{\mathrm{sp}}$ between the leader inception proximity factor K_{ℓ} and the space potential proximity factor K_{sp}.
8) For a building edge or corner, the expression for the overall proximity factor K_{p} moreover includes a term related to a leader voltage drop of normally a few meter lengths associated with the critical position corresponding to the maximum value of E_{gc}.
9) For a cylindrical building with fixed diameter, it was shown that the overall proximity factor K_{p} varies in the approximate range of 1.5 to 2.5 since the building height increased from 20 m to 100 m.
10) For an edge of a cylindrical building of 40-m diameter, it was shown that the mean critical ambient field E_{gc} dropped from 113 kV/m for a 20-m building height to 38 kV/m for a 100-m building.
11) It has been shown that for the corner of a 80 m_{*} 40 m $(\mathrm{L}_{*}\mathrm{W})$ structure, the mean critical field E_{gc} dropped from 97 kV/m for a 20-m corner height to 25 kV/m at 100-m height.
12) For any height in the range 20 m to 100 m, it has been shown that the mean critical ambient field E_{gc} for continuous leader inception is lowest for a slender rod, followed by a corner with the building edge having the highest values of E_{gc}.
13) An attractive distance ratio ADR < 1 has been introduced to express the ratio between the attractive distance of a building edge or the attraction radius of a corner to the corresponding value of a slender rod of equal height.
14) It has been shown that for a corner, ADR increases slightly with the return stroke current but is practically independent of the height of the corner above ground.
15) For a building edge, the attractive distance ratio ADR is, for the same height and return stroke current, lower than that of a corner and, furthermore, for lower currents, is more sensitive to height.
16) At an assumed threshold current of 10 kA for causing building damage, it has been approximately found that a corner would reduce the attractive radius of a slender rod by 15%, while the approximate reduction for a building edge would be 25%.
17) For a threshold current of only 5 kA, a corner causes an attractive radius reduction of approximately 20% while depending on height, the reduction due to a building edge would be in the range 30%–40%.
18) For a 100-m cylindrical building with 40-m diameter, a 10-m mast at the roof center and a 0.3-m rod at the roof edge do not provide adequate lightning protection, while according to model results, a 2-m rod at the edge provides satisfactory performance within a wide return stroke current range.
19) A 2-m rod at a structure corner has been shown to provide satisfactory lightning protection, for 20-m- and 100-m-high structures in the return stroke current range of 5 kA to 50 kA, with a better margin for the 20-m structure.

REFERENCES

[1] R. H. Golde, *Lightning Protection*. London, U.K.: Edward Arnold, 1973.
[2] M. A. Uman, *The Art and Science of Lightning Protection*. Cambridge, U.K.: Cambridge University Press, 2008.
[3] F. W. Peek, *Dielectric Phenomena in High Voltage Engineering*. New York: McGraw-Hill, 1929.
[4] F. S. Young, J. M. Clayton, and A. R. Hileman, "Shielding of transmission lines," *IEEE Trans.*, vol. S, no. 82, pp. 132–154, 1963.
[5] H. R. Armstrong and E. R. Whitehead, "Field and analytical studies of transmission line shielding," *IEEE Trans. Power App. Syst.*, vol. PAS-87, no. 1, pp. 270–281, Jan. 1968.
[6] CIGRE Working Group 33.01, "Guide to procedures for estimating the lightning performance of transmission lines," Monograph 63 Oct. 1991.
[7] *IEEE Guide for Improving the Lightning Performance of Transmission Lines*, IEEE Std. 1243-1997.
[8] W. H. Preece, "On the space protected by a lightning conductor," *Phil. Mag.*, vol. 10, p. 427, 1880.
[9] A. Schwaiger, *Der Schutzbereich von Blitzableitern (The Protection Zone of Lightning Air-Terminals)*. Munich, Germany: Oldenbourg, 1938.
[10] R. H. Lee, "Protection zone for building against lightning strokes using transmission line protection practice," *IEEE Trans. Ind. Appl.*, vol. IA-14, no. 6, pp. 465–470, Nov./Dec. 1978.
[11] R. H. Lee, "Lightning protection of buildings," *IEEE Trans. Ind. Appl.*, vol. IA-13, no. 3, pp. 236–240, May/Jun. 1979.
[12] E. R. Whitehead, "Mechanism of lightning flashover," in *EEI Res. Project RP50, Publ. 72-900*. Chicago, IL: Illinois Inst. Technol., Feb. 1971.
[13] *Standard for the Installation of Lightning Protection Systems*, NFPA Std. 780, 2004, NFPA 780 ed..
[14] *Protection Against Lightning—Part 1: General Principles*, IEC 62305-1, 2002, 1st ed.
[15] M. Darveniza, "A modification to the rolling sphere method for positioning air terminal for lightning protection of buildings," presented at the 25th Int. Conf. Lightning Protection, Rhodes, Greece, Sep. 2000, paper no. 10-10.
[16] CIGRE Task Force 33.01.03, "Lightning exposure of structures and interception efficiency of air terminals," in Monograph 118. Oct. 1997.
[17] G. Carrara and L. Thione, "Switching surge strength of large air gaps: A physical approach," *IEEE Trans. Power App. Syst.*, vol. PAS-95, no. 2, pp. 512–524, Mar./Apr. 1976.
[18] F. A. M. Rizk, "Modeling of proximity effect on positive leader inception and breakdown of large air gaps," *IEEE Trans. Power Del.*, vol. 24, no. 4, pp. 2311–2318, Oct. 2009.
[19] M. Becerra and V. Cooray, "A simplified physical model to determine the lightning upward connecting leader inception," *IEEE Trans. Power Del.*, vol. 21, no. 2, pp. 897–908, Apr. 2006.
[20] N. Goelian, P. Lalande, A. Bondiou-Clergerie, G.-L. Bachiega, A. Gazzani, and I. Gallimberti, "A simplified model for the simulation of positive-spark development in long air gaps," *J. Phys. D: Appl. Phys.*, vol. 30, pp. 2441–2452, 1997.

[21] G. Baldo, "Basic aspects of the physics concerning the development of long sparks in air," presented at the IEEE Publ. 74 CH0910-0 PWR, Summer Power Meeting, Jul. 1974.
[22] F. A. M. Rizk, "Modeling of lightning incidence to tall structures. Part 1: Theory," *IEEE Trans. Power Del.*, vol. 9, no. 1, pp. 162–171, Jan. 1994.
[23] N. I. Petrov and R. T. Waters, "Determination of the striking distance of lightning to earthed structures," in *Proc. Roy. Soc. London A*, 1995, vol. 450, pp. 589–601.
[24] E. Nasser and L. B. Loeb, "Impulse streamer branching from Lichtenberg figure studies," *J. Appl. Phys.*, vol. 34, p. 3340, 1963.
[25] F. A. M. Rizk, "Modeling of transmission line exposure to direct lightning strokes," *IEEE Trans. Power Del.*, vol. 5, no. 4, pp. 1983–1997, Oct. 1990.
[26] L. Dellera and E. Garbagnati, "Lightning stroke simulation by means of the leader progression model—Part 1: Description of the model and evaluation of exposure of free-standing structures," *IEEE Trans. Power Del.*, vol. 5, no. 4, pp. 2009–2022, Oct. 1990.
[27] G. N. Alexandrov, G. Berger, and C. Gary, "New investigations in lightning protection of substations," CIGRE, Paper no. 23/13-14 1994.
[28] M. Bernardi, L. Dellera, E. Garbagnati, and G. Sartorio, "Leader progression model of lightning: Updating of the model on basis of the recent test results," in *Proc. ICLP*, 1996, vol. 1, pp. 399–407.
[29] F. A. M. Rizk, "A model for switching impulse leader inception and breakdown of long air gaps," *IEEE Trans. Power Del.*, vol. 4, no. 1, pp. 596–606, Jan. 1989.
[30] F. A. M. Rizk, "Switching impulse strength of air insulation: Leader inception criterion," *IEEE Trans. Power Del.*, vol. 4, no. 4, pp. 2187–2194, Oct. 1989.
[31] M. Becerra and V. Cooray, "A self-consistent upward leader propagation model," *J. Phys. D.: Appl. Phys.*, vol. 39, pp. 3708–3715, 2006.
[32] M. Becerra and V. Cooray, "Time dependent evaluation of the lightning upward connecting leader inception," *J. Phys. D: Appl. Phys.*, vol. 39, pp. 4695–4702, 2006.
[33] S. Ait-Amar and G. Berger, "Attractive radius of elevated building," in *Proc. 28th Int. Conf. Lightning Protection*, Kanazawa, Japan, 2006, pp. 602–607.
[34] S. Ait-Amar and G. Berger, "A modified version of the rolling sphere theory," presented at the 29th Int. Conf. Lightning Protection, Uppsala, Sweden, 2008, paper no. 4-1.
[35] H. Singer, H. Steinbigler, and P. Weiss, "A charge simulation method for calculation of high voltage fields," *IEEE Trans. Power App. Syst.*, vol. PAS-93, no. 5, pp. 1660–1668, Sep. 1974.
[36] F. A. M. Rizk and F. Vidal, "Modeling of positive leader speed under slow front voltages—Part 1: Long air gaps," *IEEE Trans. Power Del.*, vol. 23, no. 1, pp. 296–301, Jan. 2008.
[37] Z. A. Hartono and I. Robiah, "Performance of non-standard lightning air terminals: Revisited," presented at the 29th Int. Conf. Lightning Protection, Uppsala, Sweden, 2008, paper 4–4.

Farouk A. M. Rizk (LF'09), photograph and biography not available at the time of publication.